Journal of
Radiation Protection and Research 2018;43(1):1-9
https://doi.org/10.14407/jrpr.2018.43.1.1

pISSN 2508-1888 | eISSN 2466-2461

Investigation of the Effect of kV Combinations on Image Quality for Virtual Monochromatic Imaging Using Dual-Energy CT: A Phantom Study

Pil-Hyun Jeon[1], Heejun Chung[2], Daehong Kim[3,*]

[1]Department of Radiology, Wonju Severance Christian Hospital, Wonju, Korea; [2]Korea Institute of Nuclear Nonproliferation and Control, Daejeon, Korea; [3]Department of Radiological Science, College of Health Science, Eulji University, Seongnam, Korea

ABSTRACT

Background: In this study, we investigate the image quality of virtual monochromatic images synthesized from dual-energy computed tomography (DECT) at voltages of 80/140 kV and 100/140 kV.

Materials and Methods: Virtual monochromatic images of a phantom are synthesized from DECT scans from 40 to 70 keV in steps of 1 keV under the two combinations of tube voltages. The dose allocation of dual-energy (DE) scan is 50% for both low- and high-energy tubes. The virtual monochromatic images are compared to single-energy (SE) images at the same radiation dose. In the DE images, noise is reduced using the 100/140 kV scan at the optimal monochromatic energy. Virtual monochromatic images are reconstructed from 40 to 70 keV in 1-keV increments and analyzed using two quality indexes: noise and contrast-to-noise ratio (CNR).

Results and Discussion: The DE scan mode with the 100/140 kV protocol achieved a better maximum CNR compared to the 80/140 kV protocol for various materials, except for adipose and brain. Image noise is reduced with the 100/140 kV protocol. The CNR values of DE with the 100/140 kV protocol is similar to or higher than that of SE at 120 kV at the same radiation dose. Furthermore, the maximum CNR with the 100/140 kV protocol is similar to or higher than that of the SE scan at 120 kV.

Conclusion: It was found that the CNR achieved with the 100/140 kV protocol was better than that with the 80/140 kV protocol at optimal monochromatic energies. Virtual monochromatic imaging using the 100/140 kV protocol could be considered for application in breast, brain, lung, liver, and bone CT in accordance with the CNR results.

Keywords: Dual-energy, Virtual monochromatic image, kV combination

Original Research

Received November 6, 2017
Revision December 16, 2017
Accepted December 19, 2017

Corresponding author: Daehong Kim

Department of Radiological Science, Eulji University, 553 Sanseong-daero, Seongnam 13135, Korea
Tel: +82-31-740-7494
Fax: +82-31-740-7351
E-mail: goldcollar011@gmail.com

Introduction

Computed tomography (CT) is one of the most commonly utilized methods for acquiring three-dimensional images of anatomy *in vivo*. CT generates reconstructed images as a distribution of the linear attenuation coefficient, which is averaged by the X-ray energy spectrum.

Dual-energy CT (DECT) was first developed in the 1970s [1], and the clinical application of DECT has recently been realized as a result of robust improvements in performance. The principle of DECT is the acquisition of two images of the same anatomy with different kilo-voltage (kV) settings (usually 80/140 kV). Clinically, different DECT

systems have been developed by the commercial industry, which include a rapid kV switching system with a single-layer detector [2], dual-source system with dual detectors [3], and single-source system with a dual-layer detector [4]. The DECT technique is utilized for artifact reduction [5], contrast enhancement [6], and noise reduction by mixing or synthesizing between two image sets with different spectral information [7].

An approach to generate a single set of images is to synthesize virtual monochromatic images using projection data [5, 6]. This approach was described by previous work [8, 9], which involves basis-material decomposition in the projection domain and a linear combination of the density map the basis materials. In principle, such a process can provide quantitative information and remove beam-hardening artifacts on the imaged anatomy. Beam-hardening artifact reduction is considered one of the main benefits of virtual monochromatic DECT images.

Another approach is to generate processed images from low- and high-energy images based on the image domain. The image-based virtual monochromatic images contain beam-hardening artifacts propagated from the low- and high-energy images. However, the objective of image-based monochromatic images is primarily to generate a single optimized set of images for routine diagnosis [10]. The image quality of DECT was previously evaluated in comparison to that of single-energy CT (SECT) images in routine diagnostic interpretation by Yu et al. and Alvarez and Macovski [7, 10]. They evaluated the image quality of linearly mixed images from low- (80 kV) and high-energy (140 kV) images after image reconstruction at the same total radiation dose, taking into account the effect on patient size. The results indicated that the iodine contrast-to-noise ratio (CNR) in DECT images was similar to or better than that in SECT images.

Thus, DECT techniques are useful for gaining material information by using different linear attenuation coefficients. Usually, the tube voltages are set as 80/140 kV when the DE mode is applied for a patient. Although the low energy is typically set as 80 kV because of the resulting improvement in contrast of a material, the noise level is increased at this voltage because of the increased absorption coefficients of the material. On the other hand, the high-energy scan (140 kV) provides images with lower material contrast with high-atomic-number (Z) materials, but the noise is reduced. Therefore, it is necessary to investigate different kV combinations to determine their effect on the image quality of virtual monochromatic images acquired by DE scans. Previous research on different kV combinations of 80/140 kV and 100/140 kV focused on spectral separation by means of additional filtration [11]. In their work, additional filtration for the high-energy spectrum was modified to maximize the separation between the two spectra. The results proved that the effect of filtration could allow improved DE imaging with the 100/140 kV protocol.

Prior studies focused on image quality for DECT with the 80/140 kV protocol or on spectral separation for two spectra. The reason for using 80 kV as the low energy in the DECT scan is to avoid spectral overlapping. A wider separation between spectra should improve material separation while allowing radiation dose to the patient. To achieve this, an additional filter is applied to the high energy when using 100/140 kV scanning. Therefore, it is necessary to investigate the image quality with DE scan modes such as 80/140 kV and 100/140 kV without an additional filter.

In the present study, we investigated the image quality of virtual monochromatic images synthesized from DECT scans at voltages of 80/140 kV and 100/140 kV without an additional filter at the same radiation dose. Then, the virtual monochromatic images obtained with the two scan modes were compared to SE images in terms of noise and CNR.

Materials and Methods

1. Image-based Virtual Monochromatic Imaging

Image-based virtual monochromatic imaging was reported in a previous study [10]. Virtual monochromatic images are created from reconstructed low- and high-energy images. Assuming the mass attenuation coefficients of the two basis materials at low and high energy are $\left(\frac{\mu}{\rho}\right)_i^j$, where j = L, H and i = 1, 2, the virtual monochromatic image at energy E is given by

$$\mu^j = \left(\frac{\mu}{\rho}\right)_1^j \rho_1 + \left(\frac{\mu}{\rho}\right)_2^j \rho_2, \text{ k=L, H} \quad (1)$$

where L and H represent the low and high energy, respectively, and 1 and 2 represent the two basis materials. By solving the two linear equations, one obtains the mass density of the two basis materials.

$$\rho_1 = \frac{\mu^1 \cdot \left(\frac{\mu}{\rho}\right)_2^H - \mu^H \cdot \left(\frac{\mu}{\rho}\right)_2^L}{\Delta}, \quad (2)$$

$$\rho_2 = \frac{-\mu^1 \cdot \left(\frac{\mu}{\rho}\right)_1^H + \mu^H \cdot \left(\frac{\mu}{\rho}\right)_1^L}{\Delta}, \quad (3)$$

https://doi.org/10.14407/jrpr.2018.43.1.1

where $\Delta = \left(\frac{\mu}{\rho}\right)_1^L \cdot \left(\frac{\mu}{\rho}\right)_2^H - \left(\frac{\mu}{\rho}\right)_1^H \cdot \left(\frac{\mu}{\rho}\right)_2^L$.

The virtual monochromatic image at energy E is given by

$$\mu(E) = \left(\frac{\mu}{\rho}\right)_1 (E)\rho_1 + \left(\frac{\mu}{\rho}\right)_2 (E)\rho_2. \quad (4)$$

Rewriting the linear attenuation coefficients in Equation 4 in terms of the CT number and assuming that one of the basis materials is water and the other is cortical bone, one can show that the virtual monochromatic image at energy E can be expressed as a weighted average of the images at low- and high-energy scans, which is given by

$$CT(E) = w(E)\cdot CT^L + [1 - w(E)]\cdot CT^H \quad , \quad (5)$$

where the weighting factor is given by

$$w(E) = \frac{\mu_1(E)\cdot\mu_2^H - \mu_2(E)\cdot\mu_1^H}{\mu_1^L\cdot\mu_2^H - \mu_1^H\cdot\mu_2^L}\cdot\frac{\mu_2^L}{\mu_2(E)} \quad . \quad (6)$$

Thus, the virtual monochromatic image generated from image-domain data is a linear combination of the two CT images at low and high energies, where the sum of the two weighting factors equals 1.

An optimal monochromatic energy exists that yields either the highest CNR or the lowest noise in the virtual monochromatic image. We define the standard deviations of CT numbers in the background and signal regions for low- and high-energy images as $\sigma_{j,b}$ and $\sigma_{j,s}$, respectively, where j = L, H. The contrast (the absolute difference in CT numbers between the signal region and background region) for the low- and high-energy images is denoted by C_j (j = L, H). According to the definition in a previous paper [11], the weighting factor for the highest CNR in the linearly mixed image and the corresponding maximum CNR are given by

$$w_{mCNR} = \frac{C_L(\sigma_{H,s}^2 + \sigma_{H,b}^2)}{C_L(\sigma_{H,s}^2 + \sigma_{H,b}^2) + C_H(\sigma_{L,s}^2 + \sigma_{L,b}^2)} \quad , \quad (7)$$

and

$$CNR_{\max} = \sqrt{\frac{2C_L^2}{(\sigma_{L,s}^2 + \sigma_{L,b}^2)} + \frac{2C_H^2}{(\sigma_{H,s}^2 + \sigma_{H,b}^2)}} \quad , \quad (8)$$

respectively.

The optimal weighting factor for either the lowest noise (Equation 9) or the highest CNR (Equation 10) corresponds to an optimal monochromatic energy, which can be obtained by solving either

$$w(E) = w_{m\sigma} \quad (9)$$

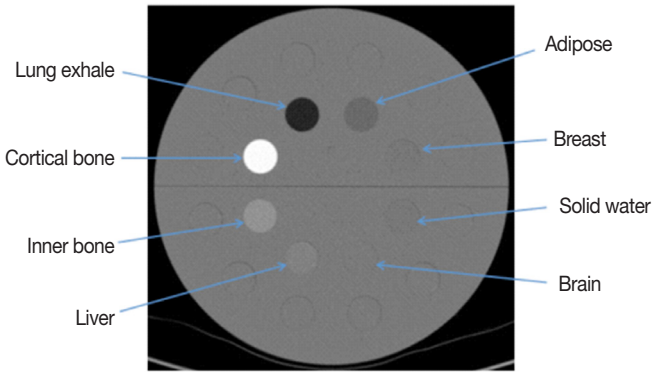

Fig. 1. HU image of Gammex 467 showing the locations of all inserts. Lung exhale, adipose, breast, solid water, brain, liver, inner bone, and cortical bone rods were inserted. The phantom was scanned using the DE and SE method.

Table 1. Human-Equivalent Materials in Gammex 467 Phantom and Their Density, Electron Density, and Effective Atomic Number

No.	Material	Density (g/m^3)	Electron density	Effective atomic number
1	Lung Exhale	1.050	1.041	7.879
2	Adipose	0.950	0.951	7.875
3	Breast	1.020	1.014	7.271
4	Solid Water	1.015	0.986	8.111
5	Brain	1.040	1.035	7.878
6	Liver	1.060	1.050	7.866
7	Inner Bone	1.133	1.086	10.895
8	Cortical Bone	1.819	1.692	14.141

for the minimum noise or

$$w(E) = w_{mCNR} \quad (10)$$

for the maximum CNR.

2. Phantom Information and Image Scan Setup

As shown in Figure 1, a tissue-characterization phantom (Gammex 467, Gammex Inc., Middleton, WI) was scanned by a CT scanner (Brilliance 64, Philips, Eindhoven, Holland) in both the SE and DE mode. Gammex 467 phantom has a diameter of 33 cm and consists of tissue substitutes such as lung exhale, adipose, breast, solid water, brain, liver, inner bone, and cortical bone. The specifications of the inserts are listed in Table 1. The phantom is scanned in the SE and DE mode in the step and shoot mode. The gantry rotation time was 1 second, and the slice thickness was 10 mm for all scans. SE scans were performed at 80, 100, 120, and 140 kV. We utilized DE scans of the 80/140 kV protocol and 100/140 kV protocol to obtain virtual monochromatic images.

Table 2. Volume Computed Tomography Dose Index ($CTDI_{vol}$) by Dose Partitioning for Single- Energy (SE) and Dual-Energy (DE) Scans

SE		DE	
kVp	$CTDI_{vol}$	kV combination	$CTDI_{vol}$
80 kV	10 mGy	80/140 kV	5/5 mGy
100 kV	10 mGy		10 mGy
120 kV	10 mGy	100/140 kV	5/5 mGy
140 kV	10 mGy		10 mGy

3. Dose Partitioning

Computed tomography dose index (CTDI) is used for dose measurement. A CTDI obtained using a 100-mm chamber is referred to as $CTDI_{100}$, which is calculated using the following equation:

$$CTDI_{100} = \frac{M \times Chamber\ length\,(mm) \times F \times TP \times CF}{N \times T}, \quad (11)$$

where M is the measured charge in roentgens, F is the exposure-to-dose conversion factor (0.78 cGy/R), TP is the correction factor for both temperature and pressure, CF is the chamber calibration factor, N is the number of slices, and T is the slice thickness (mm). The weighted CTDI ($CTDI_w$) can be obtained with a weighted $CTDI_{100}$ by using the following equation:

$$CTDI_w = \frac{1}{3}CTDI_{100,C} + \frac{2}{3}CTDI_{100,P}, \quad (12)$$

where $CTDI_{100,C}$ is the $CTDI_{100}$ measured at the center and $CTDI_{100,P}$ is the mean of the $CTDI_{100}$ measured at the 3, 6, 9, and 12 o'clock positions. Since the pitch is 1 in one scan, $CTDI_w$ is equal to $CTDI_{vol}$. A detailed description of the derivation of CTDI was reported in a previous publication [12].

Details on the dose partitioning are listed in Table 2. In the SE scan, the $CTDI_{vol}$ is 10 mGy at 80, 100, 120, and 140 kV. In DE scan, the $CTDI_{vol}$ for low- and high-energy scans is 5 mGy. Therefore, the total $CTDI_{vol}$ is 10 mGy for 80/140 and 100/140 kV [13].

4. Image Metrics

Physical metrics that influence image quality are evaluated with respect to CNR. For each DE image (80/140 kV and 100/140 kV), the CT numbers of the materials (lung exhale, adipose, breast, solid water, brain, liver, inner bone, and cortical bone) and the acryl background were measured. Virtual monochromatic images were generated from 40 to 70 keV by using Equation 2. For DE and SE images, noise is estimated by measuring the standard deviation of the region-of-interest (ROI) of the signal and background in the images of the materials. CNR is given by

$$CNR = \frac{|S - B|}{\sqrt{\sigma_s^2 + \sigma_b^2}}, \quad (13)$$

where S is the signal of the materials and B is the signal of the background. σ_s and σ_b represent the noise expressed by standard deviation. CNR is investigated for virtual monochromatic images from 40 to 70 keV and for SE images at 80, 100, 120, and 140 kV. The maximum CNR in the virtual monochromatic images is calculated using Equation 6, and the results were compared to that in the SE images.

Results and Discussion

1. Noise Evaluation

Noise is measured as a function of energy through the standard deviation of the ROI on various materials in virtual monochromatic CT images and SECT images. The trend of noise values with respect to energy is illustrated in Figure 2.

As shown in Figure 2A-2D, the noise in DE images with the 80/140 kV and 100/140 kV protocol is evaluated with respect to the virtual monochromatic energy range. Here, the virtual monochromatic images are obtained using Equation 2. For all inserts (lung exhale, adipose, breast, solid water, brain, liver, inner bone, and cortical bone), Figure 2A and 2B show plots of the noise as a function of virtual monochromatic energy with the 80/140 kV protocol. Image noise is minimized for virtual monochromatic energy ranging from 47 to 51 keV for various materials, as shown in Figure 2A and 2B. In Figure 2C and 2D, image noise is plotted for the 100/140 kV protocol. The minimum noise is observed within the energy range from 51 to 54 keV. In the SE scans, the minimum noise in the images for all inserts is observed at 120 and 140 kV. Generally, CT images are obtained with scans at a tube voltage of 120 kV. Therefore, the quality of DE images is compared to that of SE images at 120 kV. In Figure 2E and 2F, image noise is plotted for the SE scans at 80, 100, 120, and 140 kV. The mean energies of the SE scan are 41.8, 47.7, 52.5, and 56.5 keV for 80, 100, 120, and 140 kV, respectively.

The minimum noise level in virtual monochromatic images and the image noise in SE images at 120 kV are illustrated in Figure 3. Noise in DE images with the 100/140 kV protocol is less than that with the 80/140 kV protocol for all materials. Consequently, the low-energy images at 80 kV had greater

https://doi.org/10.14407/jrpr.2018.43.1.1

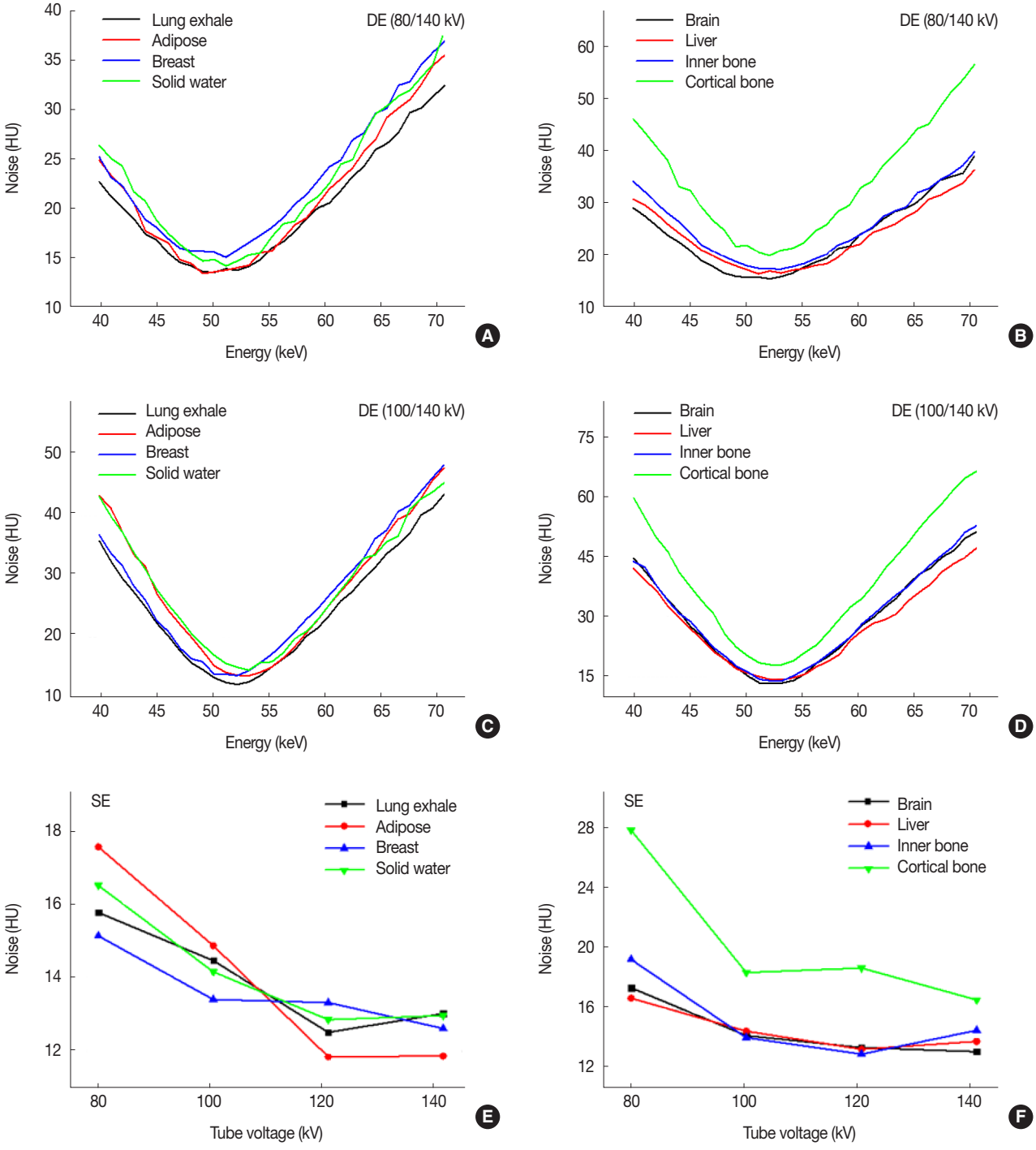

Fig. 2. Noise as a function of energy for various materials. (A) and (B) show optimal monochromatic energies in the DE image with the 80/140 kV protocol. (C) and (D) show the noise in accordance with the energy range scanned with the 100/140 kV protocol. (E) and (F) show the noise with SE scans at 80, 100, 120, and 140 kV.

noise [14-16]. When the low energy is set to 100 kV, the image noise is reduced. Therefore, the 100/140 kV scan is better than the 80/140 kV scan for achieving a reduced noise. Although the noise in DE images with the 100/140 kV protocol was reduced up to 2.63%, 1.25%, and 3.27% for lung exhale, brain, and cortical bone, the noise in SE images at 120 kV is low for adipose, breast, solid water, liver, and inner bone.

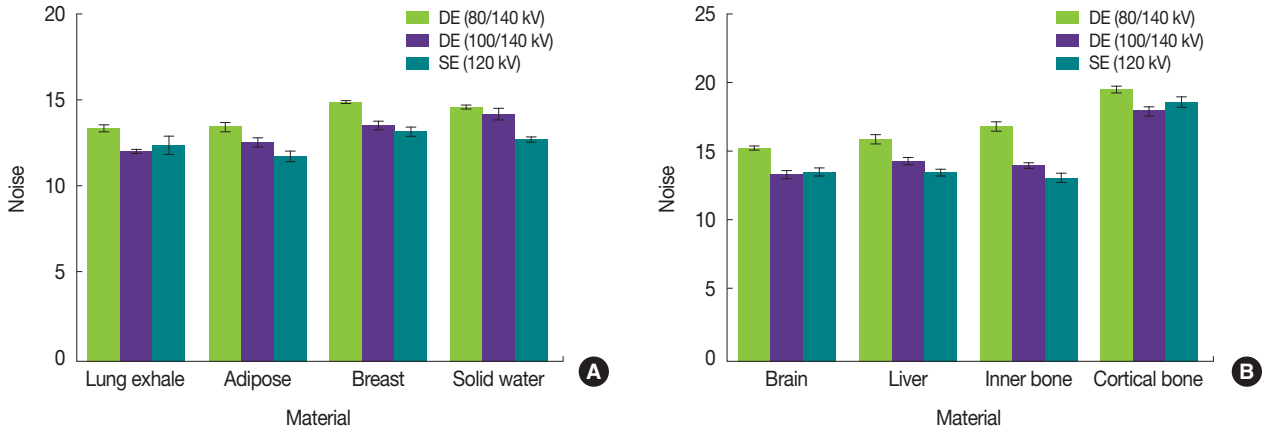

Fig. 3. Image noise in virtual monochromatic images and SE images for various materials. Overall, the image noise in DE images with the 100/140 kV protocol is less than that in DE images with the 80/140 kV protocol.

2. CNR Trend According to Energy for DE and SE images

Figure 4 shows CNR values as a function of virtual monochromatic energy for DE and SE images. DE scans with the 80/140 kV and 100/140 kV protocol are used to plot CNRs from 40 to 70 keV. SE scans are performed at 80, 100, 120, and 140 kV. In DE images, CNR is maximized in the energy range of 47-53 keV for all materials. These trends are thought to be at the minimum noise level at the optimal monochromatic energies, and this phenomenon has already been reported in previous work [10]. Although a maximum CNR exists, the CNR in SE images is higher than that in DE images. However, the maximum CNR of breast and brain in DE images is higher than that in SE images. The CNR trend of brain is different between DE and SE images because the Hounsfield unit (HU) of brain is similar to the HU of the background.

3. Maximum CNR

The maximum CNR for various materials in DE images is compared to the CNR in SE scans at 120 kV, as illustrated in Figure 5, which is derived from Equations 5 and 6. The CNR of SE images at 120 kV is measured and compared to the maximum CNR of DE images with both the 80/140 kV and 100/140 kV scans. For comparison of CNR between DE images, the results of a scan at 100/140 kV are higher than that at 80/140 kV, except for adipose and brain. As shown in Figure 5, CNR improvement in the 100/140 kV scan is 6.75%, 1.23%, 5.33%, 8.84%, 3.38%, and 2.00% for lung exhale, breast, solid water, liver, inner bone, and cortical bone. Therefore, the 100/140 kV scan is better than the 80/140 kV scan for achieving an improved CNR. The reason for this effect is that noise level is reduced when using 100 kV as the low energy.

In DECT, mixed images are created from low- and high-energy images to provide a single set of images for routine diagnosis [17]. The virtual monochromatic image is synthesized from the sum of low- and high-energy images using linear weightings. In this process, noise could be increased by summation. For comparison between the CNRs of DE and SE, we found that the CNR of SE images for various materials is slightly higher than that of DE images owing to the synthesis process of virtual monochromatic images. In addition, the effect of linear attenuation coefficients on the X-ray energy is caused by the CNR values. If 100 kV is applied as the low-energy tube voltage, image noise is reduced, and contrast between the signal and background is low. Despite this result, the CNR improvement with the 100/140 kV protocol is 7.89% and 13.33% for the breast and brain compared to the corresponding SE images.

On comparing the virtual monochromatic images obtained using the 80/140 kV and 100/140 kV protocols, the 100/140 kV protocol could be considering for application to lung exhale, solid water, liver, inner bone, and cortical bone CT in accordance with the CNR results because the CNR of DE images scanned with the 100/140 kV protocol is higher than the CNR of 80/140 scan images.

The present work demonstrates that kV combinations affect the DE virtual monochromatic image. The effect of technical factors including combinations of low and high energy was considered in this evaluation, which provides essential information for physicists, technologists, and imaging physicians regarding the image quality at an optimal polychro-

https://doi.org/10.14407/jrpr.2018.43.1.1

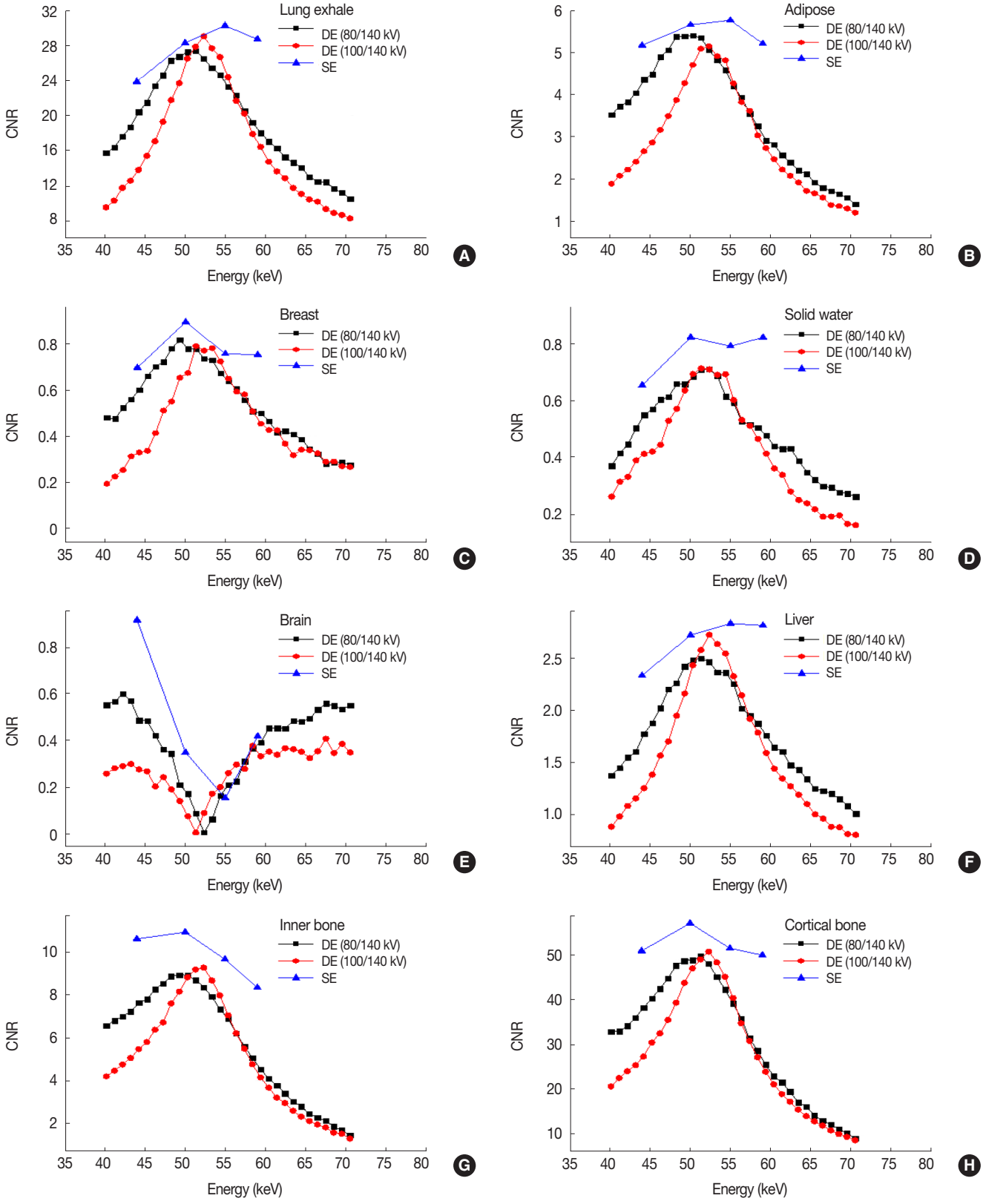

Fig. 4. (A)-(H) show a comparison of CNR value between DE and SE scans. DE scans with the 80/140 kV protocol are used to plot CNR ranging from 40 to 70 keV. The mean energies of the SE scans were 43.75, 49.72, 54.62, and 58.61 keV at 80, 100, 120, and 140 kV, respectively.

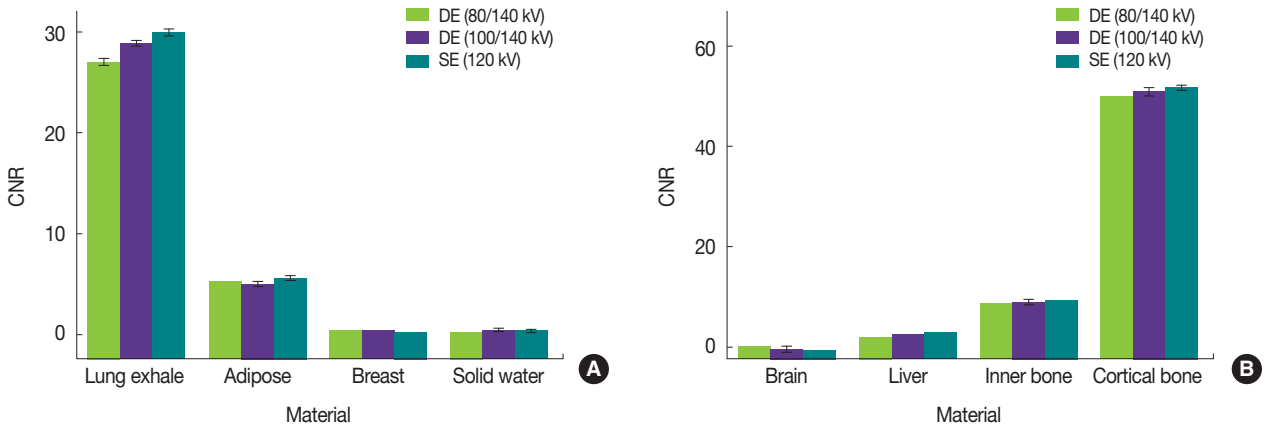

Fig. 5. (A) and (B) show the maximum CNR for various materials in DE images compared to the CNR with the SE scan at 120 kV. The CNR of SE images is higher than that of both DE images. The CNR of DE images scanned with the 100/140 kV protocol is close to the CNR of SE images.

matic tube potential for the same radiation dose.

There are some limitations of this study. We only assessed the image quality with respect to kV combinations in virtual monochromatic CT. Image quality depends on the radiation dose to the patient as well as the patient size. Further studies are needed to understand how body size and dose partitioning can influence image quality.

Conclusion

The image quality of virtual monochromatic images from DECT scan was evaluated and compared to that of SECT at the same radiation dose. The image quality of virtual monochromatic images mixed from different DECT scans was evaluated and compared to that of SECT scans at the same radiation dose. Overall, at optimal monochromatic energies, the maximum CNR with the 100/140 kV protocol was better than that with the 80/140 kV protocol. Furthermore, the maximum CNR with the 100/140 kV protocol is similar or higher than that of the SE scan at 120 kV.

Acknowledgements

This work was supported by the National Research Foundation of Korea (NRF) grant funded by the Ministry of Science and ICT (Grant No. NRF-2017R1C1B5017626).

References

1. Chiro GD, Brooks RA, Kessler RM, Johnston GS, Jones AE, Herdt JR, Sheridan WT. Tissue signatures with dual-energy computed tomography. Radiology 1979;131(2):521-523.
2. Vetter JR, Perman WH, Kalender RB, Mazess RB, Holden JE. Evaluation of a prototype dual-energy computed tomographic apparatus. II. Determination of vertebral bone mineral content. Med. Phys. 1986;13(3):340-343.
3. Flohr TG, Bruder H. Stierstorfer K, Petersilka M, Schmidt B, McCollough CH. Image reconstruction and image quality evaluation for a dual source CT scanner. Med. Phys. 2008;35(12):5882-5897.
4. Gabbai M, Leichter I, Mahqerefteh S, Sosna J. Spectral material characterization with dual-energy CT: comparison of commercial and investigative technologies in phantoms. Acta Radiol. 2015;56(8):960-969.
5. Goodsitt MM, Christodoulou EG, Larson SC. Accuracies of the synthesized monochromatic CT numbers and effective atomic numbers obtained with a rapid kVp switching dual energy CT scanner. Med. Phys. 2011;38(4):2222-2232.
6. Behrendt FF, et al. Image fusion in dual energy computed tomography: effect on contrast enhancement, signal-to-noise ratio and image quality in computed tomography. Invest. Radiol. 2009;44(1):1-6.
7. Yu L, Primak AN, McCollough CH. Image quality optimization and evaluation of linearly mixed images in dual-source, dual-energy CT. Med. Phys. 2009;36(3):1019-1024.
8. Alvarez RE, Macovski A. Energy-selective reconstruction in X-ray computerized tomography. Phys. Med. Biol. 1976;21(5):733-744.
9. Lehmann LA, Alvarez RE, Macovski A, Brody WR, Pelc NJ, Riederer SJ. Hall AL. Generalized image combinations in dual kVp digital radiography. Med. Phys. 1981;8(5):659-667.
10. Yu L, Christner JA, Leng S, Wang J, Fletcher JG, McCollough CH. Virtual monochromatic imaging in dual-source dual-energy CT: radiation dose and image quality. Med. Phys. 2011;38(12):6371-

 https://doi.org/10.14407/jrpr.2018.43.1.1

6379.
11. Primak AN, Ramirez Giraldo JC, Liu X, Yu L, McCollough CH. Improved dual-energy material discrimination for dual-source CT by means of additional spectral filtration. Med. Phys. 2009; 36(4):1359-1369.
12. Goldman LW. Principles of CT: radiation dose and image quality. J. Nucl. Med. Technol. 2007;35(4):213-225.
13. Riederer SJ, Mistretta CA. Selective iodine imaging using K-edge energies in computerized x-ray tomography. Med. Phys. 1977; 4(6):474-481.
14. Duan X, Wang J, Yu L, Leng S, McCollough CH. CT scanner x-ray spectrum estimation from transmission measurements. Med. Phys. 2011;38(2):993-997.
15. Shkumat NA, Siewerdsen JH, Dhanantwari AC, Williams DB, Richard S, Paul NS, Yorkston J, Van Metter R. Optimization of image acquisition techniques for dual-energy imaging of the chest. Med. Phys. 2007;34(10):3904-3915.
16. Wang X, Meier D, Mikkelsen S, Maehlum GE, Wagenaar DJ, Tsui BMW, Patt BE, Frey EC. MicroCT with energy-resolved photon-counting detectors. Phys. Med. Biol. 2011;56(9):2791-2816.
17. Kim KS, Lee JM, Kim SH, Kim KW, Kim SJ, Cho SH, Han JK, Choi BI. Image fusion in dual-energy computed tomography for detection of hypervascular liver hepatocellular carcinoma phantom and preliminary studies. Invest. Radiol. 2010;45(3):149-157.